Thermal–economic modelling and optimization of gas engine-driven heat pump systems

S Sanaye* and **M Chahartaghi**
Energy Systems Improvement Laboratory (ESIL), Iran University of Science and Technology, Tehran, Iran

The manuscript was received on 9 November 2009 and was accepted after revision for publication on 11 January 2010.

DOI: 10.1243/09576509JPE920

Abstract: Gas engine-driven heat pump (GEHP) modelling and optimization are presented in this article. Heat pump cycle modelling included a compressor, condenser, evaporator, expansion valve, and gas engine to drive the compressor. To validate the modelling output results, they were compared with experimental results, and acceptable difference per cent points were obtained and reported.

For the optimal design of GEHPs, the total annual cost (sum of operating and investment costs) was defined as the objective function in terms of technical and economic parameters of the system. The genetic algorithm optimization technique was used to obtain the design parameters at the minimum total cost of the system. Eight design parameters of the system (condenser and evaporator pressures in cooling and heating modes, inlet air mass flowrate to indoor and outdoor heat exchangers, and gas engine rotational speed in cooling and heating modes) were selected. The values of the design parameters for a case study were obtained and reported when the total annual cost of the system was minimum. Furthermore, at that system optimal design point, the investment and operating costs were found to be 64.23 per cent and 35.67 per cent of the total cost, the fuel consumptions of the gas engine were 0.956 and 0.658 kg/h, respectively, and the coefficients of performance (COPs) of the GEHP were 1.61 and 1.64 in the cooling and heating modes, respectively. The variation of optimum design parameters in various cooling and heating loads was studied. Finally, sensitivity analysis and the change in design parameters with the change in fuel price and investment cost were studied.

Keywords: gas engine-driven heat pump, vapour compression refrigeration cycle, gas engine, thermal–economic modelling, optimization, genetic algorithm

1 INTRODUCTION

Heat pumps are important for the cooling and heating of buildings. Heat pumps with a vapour compression refrigeration cycle include two low (evaporator) and high (condenser) temperature levels. They usually have two heat exchangers inside and outside the building. Indoor and outdoor heat exchangers are the condenser and evaporator in the heating mode, and the evaporator and condenser in the cooling mode, respectively. A reversing valve switches the position of the evaporator and the condenser in the heating and cooling modes [**1**].

Based on the type of driving engine used for rotating the compressor shaft (an electrical motor or a gas engine), heat pumps are categorized into electrical heat pumps and gas engine-driven heat pumps (GEHPs) [**2**]. Considering the lower price of natural gas in comparison with electricity, these systems are used, especially in regions with reliable resources of natural gas with low operational cost [**3**, **4**].

A GEHP system mainly consists of two parts: a heat pump system (consisting of a compressor, condenser, expansion valve, and evaporator) and a gas engine.

Considering the importance of using GEHPs in air conditioning equipment, modelling and optimizing these systems are essential from the technical and economic points of view.

**Corresponding author: Energy Systems Improvement Laboratory (ESIL), Mechanical Engineering Department, Iran University of Science and Technology, Narmak, Tehran 16844, Iran.*
email: sepehr@iust.ac.ir

In some models, individual components such as the evaporator, compressor, condenser, expansion valve, and gas engine were studied in detail, and then the integrated system was analysed; in other models, system operating parameters such as COP and heating/cooling capacities were studied without a detailed analysis of system components.

Hepbasli *et al.* [**5**] reviewed GEHP systems for residential and industrial applications. In their study, the historical development of GEHP systems was briefly given and the operation of these systems was described. GEHPs were then modelled for system performance analysis (the capacity of heat exchangers and the COP of GEHP) using energy and mass conservation equations.

Zhang *et al.* [**2**] established a steady-state model to estimate the operation of GEHPs. Models of the compressor and internal combustion engine were developed based on manufacturers' data and experimental results, while a model of heat exchangers was obtained from the mass and energy conservation equations. Finally, system modelling was validated by comparing the modelling outputs with the experimental data.

Nowakowski *et al.* [**6**] discussed the field testing of high-efficiency, natural gas, engine-driven heating and the cooling system for residential and light commercial applications. A product description was provided and the basic operating principles were discussed. Field test results were presented, which confirm high seasonal operating efficiencies with heating and cooling COP ranges, depending on climate, application, and user comfort preference. Operating costs, comfort considerations, and life considerations were also briefly addressed.

Yagyu *et al.* [**7**, **8**] tested the performance of a gas engine-driven Stirling heat pump. They estimated the total COP, and stated that if the heat pump system could be pressurized up to 5 MPa, COP would be improved.

The technical and economic optimization of thermal systems has been a subject of interest for many years. Wall [**9**, **10**] presented a method for the technoeconomic optimization of a vapour compression refrigeration cycle. He considered the total annual cost of a heat pump, including the sum of the initial investment and power consumption costs, as the objective function. Furthermore, equipment cost functions were introduced, and the minimum value of the objective function was obtained using the Lagrange multipliers method.

Cammarata *et al.* [**11**] also used a thermoeconomic method to optimize air conditioning systems. Their objective function included parameters such as inlet fresh air mass flowrate, coefficient of performance, and the inlet water temperature of the cooling and heating coils. The global optimum value of the objective function was reached by applying the mathematical direct search method.

Sanaye and Malekmohammadi [**12**] presented a method of obtaining the thermal and economic optimum design of air conditioning systems with a vapour compression refrigeration cycle. They presented an optimization procedure with the total cost of the system (including the sum of the initial investment and electricity costs) per unit cooling load of the system as the objective function. By changing the values of condenser and evaporator temperature levels and air mass flowrate, the objective function was minimized using the Lagrange multipliers method.

Selbas *et al.* [**13**] performed the technical and economic optimization of the vapour compression refrigeration cycle. In their method, optimum values of heat transfer surface area for heat exchangers as well as subcooling and superheating degrees were obtained for various operating conditions of the system. Furthermore, variations in equipment cost with subcooling and superheating degrees were investigated.

In this article, the heat pump cycle is modelled using thermodynamic characteristics of the components and empirical relations. A model was applied to obtain the gas engine power based on variations in crank angle. Using the heat pump and gas engine models simultaneously, GEHP operating characteristics, such as COP and fuel consumption, were obtained in both cooling and heating modes of operation. The capacity of heat exchangers, the compressor power consumption, the efficiencies of GEHP elements, and the technical characteristics of the system can be obtained using the presented model.

In the optimization section, the total annual cost of the system, including the initial investment cost as well as the operating cost (electricity and fuel costs), was considered as the objective function. Considering the fact that the system operates in both hot and cold seasons during a year, the annual operating cost includes the costs of operation during both heating and cooling modes.

The optimum value of the objective function was obtained by changing the values of eight selected decision variables in the permissible operating ranges, considering the constraints of the problem. The optimum values of design parameters were presented in both cooling and heating modes. Furthermore, other technical characteristics of the system such as COP, fuel consumption, and elements' efficiency were computed at the optimal design condition.

The values of minimum total cost and the corresponding optimal design parameters were presented at various cooling and heating capacities. Finally, the sensitivity analysis of the change in the optimum values of decision variables with the fuel price and initial investment cost was performed. The optimization method was based on the genetic algorithm (GA) technique.

In summary, this article contributes the following in the modelling and optimization of GEHPs.

1. Proposing a heat pump model with the capability of predicting the operating characteristics of the heat pump cycle as well as evaluating the validity of modelling outputs with experimental results.
2. Performing the detailed analysis of a gas engine and its effects of geometrical and technical specifications on optimum design parameters and estimating losses such as heat loss, friction loss, mass loss, and exhaust loss.
3. Proposing a GEHP model (considering the simultaneous operation of both heat pump and gas engine systems) to compute COP and fuel consumption in both cooling and heating modes of operation.
4. Introducing an objective function as the sum of the initial investment and operating costs in both cooling and heating operating modes and introducing eight independent variables with their permissible ranges. Furthermore, computing the values of design variables for which the minimum value of the objective function was obtained (optimum values of design parameters) using the GA optimization technique at various values of cooling/heating capacity.
5. Investigating the effects of change in the investment and fuel costs on the value of the objective function as well as optimum design values (sensitivity analysis).
6. Computing and drawing the energy flow diagram for the GEHP system.

2 THERMAL MODELLING OF GEHPS

In this section, the heat pump cycle (vapour compression refrigeration cycle) and the gas engine cycle are modelled. Figure 1 shows the schematic view of a GEHP and Fig. 2 shows the T–s diagram of the vapour compression refrigeration cycle.

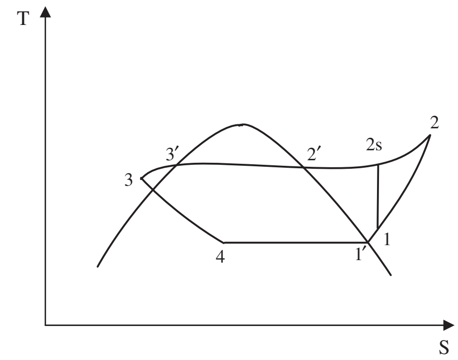

Fig. 2 T–s diagram of a vapour compression refrigeration cycle

2.1 Compressor

The compressor power consumption was obtained from

$$\dot{W}_{\mathrm{comp}} = \dot{m}_{\mathrm{r}} w_{\mathrm{comp}} = \dot{m}_{\mathrm{r}}\,(h_2 - h_1) = \dot{m}_{\mathrm{r}}\left(\frac{h_{2\mathrm{s}} - h_1}{\eta_{\mathrm{s}}}\right) \tag{1}$$

The refrigerant mass flowrate was computed from

$$\dot{m}_{\mathrm{r}} = \eta_{\mathrm{v}}\,\rho_1 \frac{V_{\mathrm{comp}}\,N_{\mathrm{comp}}}{60} \tag{2}$$

The volumetric efficiency for the scroll compressor with R407C was computed as a function of the compression ratio [**14**]

$$\eta_{\mathrm{v}} = a_0 + a_1\left(\frac{P_{\mathrm{dis}}}{P_{\mathrm{suc}}}\right), \quad 2.5 \leqslant \frac{P_{\mathrm{dis}}}{P_{\mathrm{suc}}} \leqslant 6.5 \tag{3}$$

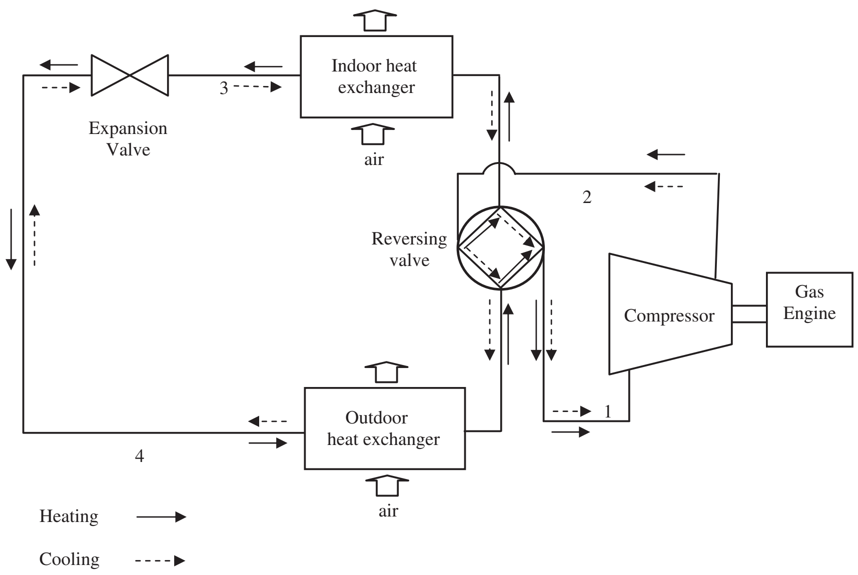

Fig. 1 Schematic diagram of a typical GEHP cycle

The following relation was used to compute the isentropic efficiency of the scroll compressor in the mentioned range of compression ratio [14]

$$\eta_s = b_0 + b_1\left(\frac{P_{dis}}{P_{suc}}\right) + b_2\left(\frac{P_{dis}}{P_{suc}}\right)^2 \tag{4}$$

2.2 Condenser

The heat transfer rate in the condenser was computed from

$$\dot{Q}_{con} = \dot{m}_r q_{con} = \dot{m}_r(h_2 - h_3) \tag{5}$$

In the steady state, the heat absorbed by air passing through the condenser is equal to the heat released from the refrigerant, and was computed from

$$\begin{aligned}\dot{Q}_{con} &= \dot{m}_{a,con}\, c_{p,a}\,(T_{a,con,o} - T_{a,con,i})\\ &= \rho_{a,con}\,\dot{V}_{a,con}\,c_{p,a}(T_{a,con,o} - T_{a,con,i})\end{aligned} \tag{6}$$

2.3 Expansion valve

In the isenthalpic throttling process [15]

$$h_3 = h_4 \tag{7}$$

In steady flow condition, the values of mass flowrate in the expansion valve and the compressor are the same ($\dot{m}_{exv} = \dot{m}_r$).

2.4 Evaporator

The heat transfer rate in the refrigerant side of the evaporator was computed from

$$\dot{Q}_{eva} = \dot{m}_r q_{eva} = \dot{m}_r\,(h_1 - h_4) \tag{8}$$

In steady flow condition, $\dot{m}_r$ is constant in the cycle and is equal to the mass flowrate in the compressor. Also, the heat extracted from the air by the evaporator is equal to the heat absorbed by the refrigerant, and was obtained from

$$\begin{aligned}\dot{Q}_{eva} &= \dot{m}_{a,eva}\, c_{p,a}\,(T_{a,eva,i} - T_{a,eva,o})\\ &= \rho_{a,eva}\,\dot{V}_{a,eva}\,c_{p,a}(T_{a,eva,i} - T_{a,eva,o})\end{aligned} \tag{9}$$

2.5 Gas engine

A spark ignition internal combustion gas engine was used to drive the compressor of the heat pump with the vapour compression cycle.

The heat release process during the combustion of an air and fuel mixture in the cylinder was computed as a function of crank angle [16, 17]

$$x = 1 - \exp\left[-\left(\frac{\theta - \theta_s}{\theta_d}\right)^n\right], \quad \theta_s < \theta < \theta_s + \theta_d \tag{10}$$

The values of θ_s, θ_d, and n were obtained from a wide range of experimental data for spark ignition engines.

Assuming that the gases in the cylinder are ideal gases and by differentiation of the above equation in terms of crank angle (θ), using the first law of thermodynamics in differential form, and considering the heat and mass losses in the engine cylinder, the following four ordinary differential equations were obtained in dimensionless form. The values of pressure, output work, heat loss, and mass of gases in the cylinder were obtained by solving these four equations simultaneously

$$\begin{aligned}\frac{d\tilde{P}}{d\theta} &= -\gamma\frac{\tilde{P}}{\tilde{V}}\frac{d\tilde{V}}{d\theta} + \frac{(\gamma-1)}{\tilde{V}}\\ &\quad\times\left[\tilde{Q}\frac{dx}{d\theta} - \tilde{\alpha}(1+\beta\tilde{V})\left(\frac{\tilde{P}\tilde{V}}{\tilde{m}} - \tilde{T}_w\right)\right] - \gamma\frac{C_0\tilde{P}}{\omega_{ge}}\end{aligned} \tag{11}$$

$$\frac{d\tilde{W}}{d\theta} = \tilde{P}\frac{d\tilde{V}}{d\theta} \tag{12}$$

$$\frac{d\tilde{Q}_{loss}}{d\theta} = \tilde{\alpha}(1+\beta\tilde{V})\left(\frac{\tilde{P}\tilde{V}}{\tilde{m}} - \tilde{T}_w\right) \tag{13}$$

$$\frac{d\tilde{m}}{d\theta} = -\frac{C_0\tilde{m}}{\omega_{ge}} \tag{14}$$

The dimensionless parameters in the above relations are listed in Table 1.

Table 1 Dimensionless factors in engine modelling [16]

Parameter	Value
Dimensionless pressure	$\tilde{P} = \dfrac{P}{P_1}$
Dimensionless volume	$\tilde{V} = \dfrac{V}{V_1} = \left[1 + \dfrac{r_c - 1}{2}(1-\cos\theta)\right]/r_c$
Dimensionless temperature	$\tilde{T} = \dfrac{T}{T_1}$
Dimensionless heat loss	$\tilde{Q}_{loss} = \dfrac{Q_{loss}}{P_1 V_1}$
Dimensionless heat of combustion	$\tilde{Q} = \dfrac{Q_{in}}{P_1 V_1} = \dfrac{1}{1+\mathrm{AF}}\dfrac{q_{LHV}}{RT_1}\eta_{comb}\,\eta_{v,ge}$
Dimensionless mass of gases inside the cylinder	$\tilde{m} = \dfrac{m}{m_1}$
Dimensionless heat transfer coefficient	$\tilde{\alpha} = \dfrac{\alpha T_1(A_0 - 4V_0/b)}{P_1 V_1 \omega_{ge}}$
β factor	$\beta = \dfrac{4V_1}{b(A_0 - 4V_0/b)}$
Blow-by factor	$C_0 = \dfrac{\dot{m}_{loss}}{m}$

Subscript '1' in Table 1 refers to the state of gases at the beginning of the compression process; $\omega_{ge} = 2\pi N_{ge}/60$ is the engine frequency (rad/s).

At the end of the combustion process, the indicated work for the cycle was computed, and the indicated thermal efficiency (η_{th}) was obtained from

$$\eta_{th} = \frac{\tilde{W}}{\tilde{Q}} \tag{15}$$

2.6 Heat pumps and GEHPs

After estimating engine indicated work and thermal efficiency depending on spark angle (time), the compressor power consumption and engine indicated power output ($\dot{W}_{ge,i}$) were then related using the following equation

$$\dot{W}_{comp} = \dot{W}_{ge,i}\ \eta_m\ \eta_{belt} \tag{16}$$

$$\eta_{th} = \frac{\dot{W}_{ge,i}}{\dot{Q}_{in}} = \frac{\dot{W}_{ge,i}}{\dot{m}_{fuel}\ q_{LHV}\ \eta_{comb}} \tag{17}$$

Combining the above equations, the fuel mass flowrate can be computed from

$$\dot{m}_{fuel} = \frac{\dot{W}_{ge,i}}{\eta_{th}\ \eta_{comb}\ q_{LHV}} = \frac{\dot{W}_{comp}}{\eta_m\ \eta_{belt}\ \eta_{th}\ \eta_{comb}\ q_{LHV}} \tag{18}$$

The ratio of compressor rotational speed to engine rotational speed (K_{belt}) was defined in the form

$$K_{belt} = \frac{N_{comp}}{N_{ge}} \tag{19}$$

Furthermore, the values of COP of the GEHP in cooling and heating modes were obtained from

$$\mathrm{COP_c} = \frac{\dot{Q}_{eva,c}}{\dot{Q}_{in,c}} = \frac{\dot{Q}_{eva,c}}{\dot{m}_{fuel,c}\ q_{LHV}\ \eta_{comb}} \tag{20}$$

Combining equations (17), (18), and (20), one has

$$\begin{aligned}\mathrm{COP_c} &= \frac{\dot{Q}_{eva,c}}{\dot{W}_{comp,c}}\ \eta_{m,c}\ \eta_{belt}\ \eta_{th,c} \\ &= \frac{q_{eva,c}}{w_{comp,c}}\ \eta_{m,c}\ \eta_{belt}\ \eta_{th,c} \\ &= \mathrm{COP_{HP,c}}\ \eta_{m,c}\ \eta_{belt}\ \eta_{th,c}\end{aligned} \tag{21}$$

$$\mathrm{COP_h} = \frac{\dot{Q}_{con,h}}{\dot{Q}_{in,h}} = \frac{\dot{Q}_{con,h}}{\dot{m}_{fuel,h}\ q_{LHV}\ \eta_{comb}} \tag{22}$$

and from equations (17), (18), and (22) one has

$$\begin{aligned}\mathrm{COP_h} &= \frac{\dot{Q}_{con,h}}{\dot{W}_{comp,h}}\ \eta_{m,h}\ \eta_{belt}\ \eta_{th,h} \\ &= \frac{q_{con,h}}{w_{comp,h}}\ \eta_{m,h}\ \eta_{belt}\ \eta_{th,h} \\ &= COP_{HP,h}\ \eta_{m,h}\ \eta_{belt}\ \eta_{th,h}\end{aligned} \tag{23}$$

3 OPTIMIZATION

3.1 Objective function and decision variables

The objective function was defined as the total annual cost of the system including initial investment (C_{inv}) and operating (C_{opr}) costs

$$C_{tot} = C_{inv} + C_{opr} \tag{24}$$

The initial investment cost of the components of the GEHP system was computed as

$$C_{inv} = C_{comp} + C_{ihx} + C_{exv} + C_{ohx} + C_{ge} \tag{25}$$

Considering the fact that GEHPs work in both cooling and heating modes (at different operating conditions such as refrigerant pressure, mass flowrate, and efficiency) during a year, the cost of system components must be determined based on the working hours of the cooling and heating modes in a year. Therefore, the ratios between the annual operating hours of the system in cooling and heating modes to the total annual operating hours of the system in a year (τ_c and τ_h) were defined to determine the initial investment cost of the components in each operating mode. Then the weighted average of a component cost (C_i) during the year was computed from

$$C_i = \tau_c C_{i,c} + \tau_h C_{i,h} \tag{26}$$

The operating cost of the system was also obtained from

$$C_{opr} = C_{fuel} + C_{el} \tag{27}$$

Based on the model presented by Wall [**9**, **10**], the heat pump element costs were computed (Appendix 2).

The indoor and outdoor heat exchangers were the condenser and evaporator in the heating mode, and the evaporator and condenser in the cooling mode, respectively.

The purpose of optimization is to minimize the system total cost (C_{tot}). In this article, various operating parameters of the system were selected as design parameters. These parameters include evaporator pressures in cooling and heating modes ($P_{eva,c}$ and $P_{eva,h}$), condenser pressures in cooling and heating modes ($P_{con,c}$ and $P_{con,h}$), air mass flowrate in the indoor heat exchanger ($\dot{m}_{a,ihx}$),air mass flowrate in the outdoor heat exchanger ($\dot{m}_{a,ohx}$), and gas engine rotational speed in cooling and heating modes ($N_{ge,c}$ and $N_{ge,h}$). The minimum value of the total annual cost was obtained considering the permissible range of system operation in cooling and heating modes. The optimization was performed by applying the GA method.

The objective function was defined as a function of the mentioned eight design parameters

$$C_{\text{tot}} = f(P_{\text{eva,c}}, P_{\text{eva,h}}, P_{\text{con,c}}, P_{\text{con,h}}, \dot{m}_{\text{a,ihx}}, \dot{m}_{\text{a,ohx}}, N_{\text{ge,c}}, N_{\text{ge,h}}) \quad (28)$$

The algorithm of computations to minimize the objective function is shown in Fig. 3.

3.2 Optimization method (GA)

The GA technique was used to optimize the objective function in this article. GA is a general-purpose search method and a non-deterministic optimization technique based on the principles of evolution observed in nature [**18**].

In the GA used in this article, the selection function was stochastic uniform and the crossover fraction was 0.8. The termination criterion of the algorithm was the difference in the error value equal to 10^{-6} compared to the previous generation that achieved at about 220 generations (Fig. 4). Considering the unchanged value of the objective function in the next iteration, the optimization computation was terminated.

3.3 System constraints

In the optimization process, the design parameters or decision variables change in permissible ranges. The optimum values of the design parameters minimize the total annual cost of the system (C_{tot}).

The following constraints were applied in the optimization procedure.

1. The condenser mean temperature has to be at least 5 °C greater than the surrounding air temperature,

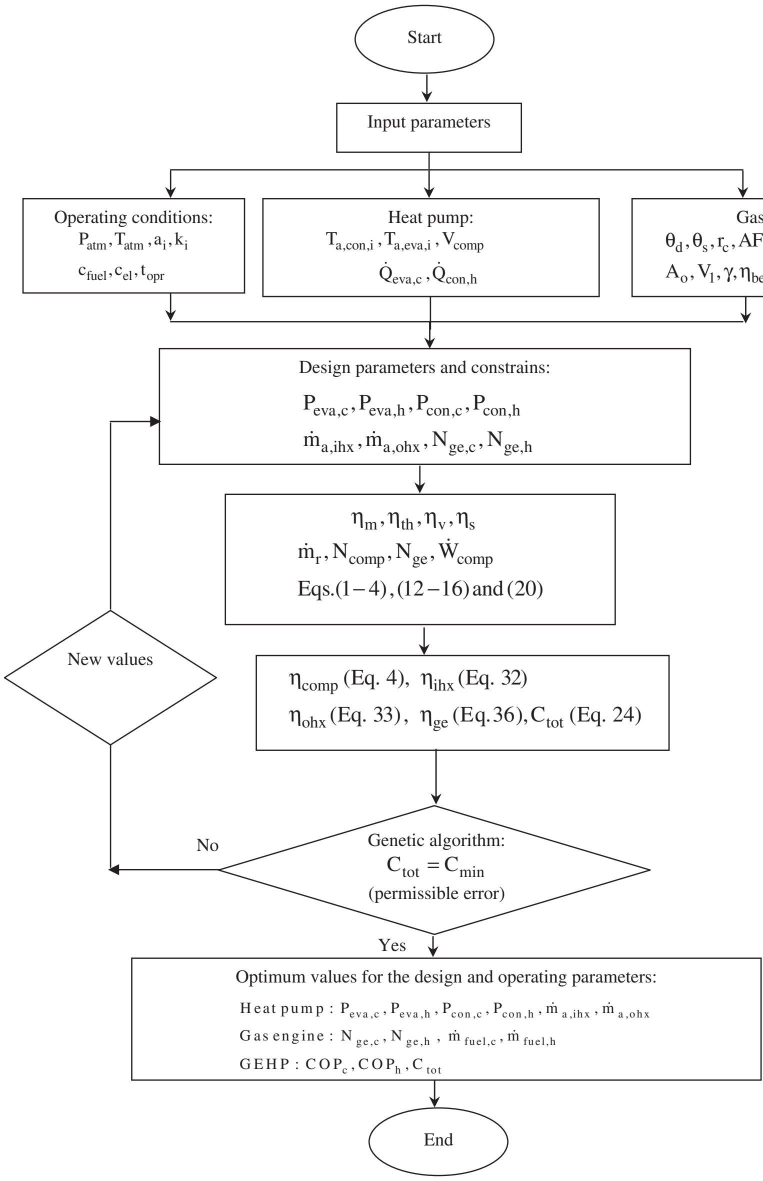

Fig. 3 Modelling and optimization algorithm

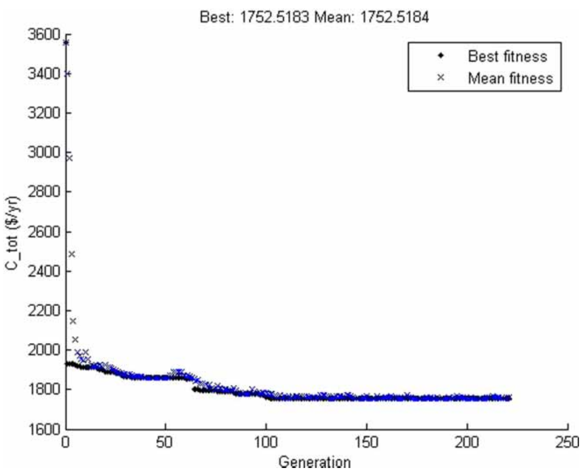

Fig. 4 Variation in the objective function towards the final optimum value for the case study (ESIL) explained in section 4

and the evaporator mean temperature has to be at least 5 °C lower than the surrounding air temperature [**19**]. Thus, according to the permissible pressure ratio of the compressor and the limitation of the air temperature surrounding the evaporator and condenser, the permissible operating pressures of the condenser and evaporator were determined.

2. The typical range of scroll compressor pressure ratio was $2.5 \leqslant P_{dis}/P_{suc} \leqslant 6.5$ [**14**]; therefore, the typical pressure ranges of R407C refrigerant in the evaporator and condenser in the cooling and heating modes were as follows.
   (a) $2 \leqslant P_{eva} \leqslant 5.5$ bar;
   (b) $15 \leqslant P_{con} \leqslant 30$ bar.
3. The typical range of air mass flowrate in indoor and outdoor heat exchangers was $1 \leqslant \dot{m}_a \leqslant 10$ kg/s [**20**].
4. The efficiency of all elements has to be in the range of $0 < \eta_i < 1$.
5. The typical range for gas engine rotational speed was $1200 \leqslant N_{ge} \leqslant 2600$ r/min [**20**].

The optimization algorithm is presented in Fig. 3.

4 CASE STUDY

Based on the presented modelling and optimization procedure, a typical GEHP system was modelled and optimized for the estimated cooling and heating loads of the Energy Systems Improvement Laboratory (ESIL).

The estimated cooling ($\dot{Q}_{eva,c}$) and heating ($\dot{Q}_{con,h}$) capacities for the case study were 12.5 kW and 18.5 kW, respectively.

A supplementary programme was developed to compute the properties of R407C refrigerant in the main modelling and optimization programme.

For superheating in the evaporator and subcooling in the condenser, the average typical values (5 °C) were considered based on the data provided in references [**19**] and [**21**].

The annual cooling and heating time periods were 40 per cent and 60 per cent of the year based on local atmospheric conditions; therefore, τ_c and τ_h were 0.4 and 0.6, respectively. Furthermore, fuel consumption was computed based on 1600 (h/year) and 2400 (h/year) for cooling and heating modes, respectively. The fuel and electricity costs were also 0.01 $/kWh (0.1 $/m3) and 0.04 $/kWh. The lower heating value of fuel was 44 700 (kJ/kg). The stoichiometric air to fuel ratio was 16.5.

Design conditions in Tehran (the capital of Iran), including the mean temperature and relative humidity, were considered as 35 °C (considering 22 °C indoor temperature) and 20 per cent in the cooling mode, and 5 °C (considering 24 °C indoor temperature) and 45 per cent in the heating mode. The barometric pressure was 85 kPa.

The interest rate (r) and the depreciation time of components (n_i) were considered as 10 per cent and 15 years, respectively.

5 DISCUSSION AND RESULTS

5.1 Evaluating the validity of modelling results

5.1.1 *Evaluating the validity of the heat pump cycle model*

To evaluate the heat pump cycle model, about 30 tests were performed on the installed GEHP for various cooling/heating capacities. The modelling and test results were compared in each test run and the mean difference per cent points for compressor power consumption ($\dot{W}_{comp} = Q_{cond} - Q_{eva}$), evaporator cooling capacity, and condenser heating capacity were 4 per cent, 2.9 per cent, and 1.6 per cent, respectively.

The temperature and velocity of air passing over evaporator/condenser tubes were measured by appropriate thermometer/thermal bulb sensors. The cooling and heating capacities of the system were computed by measuring the outlet air temperature of heat exchangers.

5.1.2 *Evaluating the validity of the gas engine cycle model*

To validate the presented model and developed software program for the gas engine cycle, modelling outputs were compared with the corresponding reported values in reference [**16**] for the same input values.

The input parameters mentioned in reference [**16**], and the modelling output results as well as the

Table 2 Comparison of the results for the presented engine modelling and the corresponding values given in reference [**16**] with the same input values

Input parameters			Value
r_c			10
γ			1.3
θ_s			−40
θ_d			40
$\tilde{Q}$			20
$\boldsymbol{n}$			4
$\tilde{\alpha}$			0.2
β			1.5
$\tilde{T}_w$			1.2
C_o			0.8
ω_{ge}			200
Output parameters	Presented model	Reference [**16**]	Difference (%)
$\tilde{P}$	68.67	68.55	0.18
$\tilde{W}$	8.72	8.69	0.34
$\tilde{Q}_{loss}$	4	3.97	0.76
$\tilde{m}$	0.976	0.9752	0.1
η_{th}	0.436	0.4345	0.34

corresponding results presented in reference [**16**] are shown in Table 2. The results show good agreement and validation of the gas engine cycle model.

5.1.3 Evaluating the validity of the GEHP model

To evaluate the validity of the whole GEHP model, about 40 experimental tests were performed on a GEHP unit in various cooling and heating capacities. The cooling and heating capacities of the system were computed by measuring the outlet air temperature of heat exchangers. The COP of the GEHP was computed by measuring system fuel consumption by a gas flow meter. The modelling input parameters were mentioned in section 4 for the installed and tested GEHP system.

The average difference per cent points between the modelling results and the empirical tests for cooling and heating capacity, COP, and fuel consumption were about 4.6 per cent, 2.5 per cent, 7.5 per cent, and 4.5 per cent, respectively, which showed the accepted output results for GEHP system modelling.

5.2 Optimization results

For the case study (ESIL) mentioned in section 4, the minimum value of the objective function (C_{tot}) was obtained by a change in design parameters in permissible ranges. The values of design parameters for which the minimum total cost was achieved were obtained. The variation of the numerical value for the objective function with number of generations towards the minimum value is shown in Fig. 4. The best fitness curve shows the best function value in each generation which changes in each number of iteration and the mean fitness points on this curve illustrate the mean value of the objective function at that step. The optimum values of the design parameters, at the minimum total cost of the system, are presented in Table 3.

The cost of system components at the optimum design point is shown in Fig. 5, and the operating parameters of the optimized system (with optimum design parameters) in the cooling and heating modes of operation are presented in Table 4.

Furthermore, the modelling and optimizing results at various cases of cooling/heating capacities listed in Table 5 are shown in Figs 6 to 13.

Table 3 Optimum values of design parameters

Parameter	Unit	Value
Evaporator pressure in cooling mode ($P_{eva,c}$)	bar	5.5
Evaporator pressure in heating mode ($P_{eva,h}$)	bar	4.27
Condenser pressure in cooling mode ($P_{con,c}$)	bar	18.98
Condenser pressure in heating mode ($P_{con,h}$)	bar	17.38
Inlet air mass flowrate to indoor heat exchanger ($\dot{m}_{a,ihx}$)	kg/s	1.504
Inlet air mass flowrate to outdoor heat exchanger ($\dot{m}_{a,ohx}$)	kg/s	2.51
Gas engine rotational speed in cooling mode ($N_{ge,c}$)	r/min	1576
Gas engine rotational speed in heating mode ($N_{ge,h}$)	r/min	1671

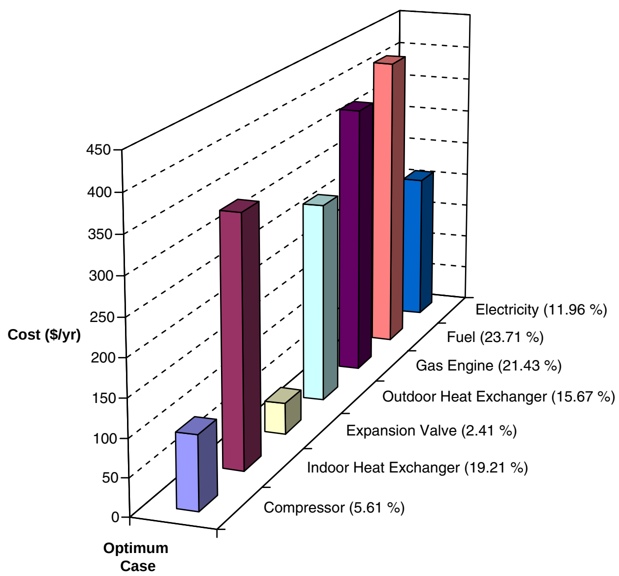

Fig. 5 Cost for the components at the optimal design point (the minimum total cost) for the case study (ESIL) explained in section 4

Table 4 Numerical values of the operating parameters from system modelling at the optimal design point (with optimum values of the design parameters)

Parameter	Unit	Equation number	Cooling	Heating
Compressor volumetric efficiency (η_v)	%	(3)	95.64	93.9
Compressor isentropic efficiency (η_{comp})	%	(4)	78.6	74.28
Compressor power consumption ($\dot{W}_{comp}$)	kW	(1)	2.56	3.73
Compressor rotational speed (N_{comp})	r/min	(2)	1785	2717
Indoor heat exchanger efficiency (η_{ihx})	%	(32)	42.97	64.86
Outdoor heat exchanger efficiency (η_{ohx})	%	(33)	52.42	60.13
Outdoor heat exchanger capacity ($\dot{Q}_{ohx}$)	kW	(5) and (8)	15.06	14.77
Gas engine power output ($\dot{W}_{ge}$)	kW	(39)	2.69	3.93
Gas engine efficiency (η_{ge})	%	(36)	34.69	34.86
Fuel consumption mass flowrate ($\dot{m}_{fuel}$)	kg/h	(18)	0.658	0.956
Coefficient of performance (COP)	–	(21) and (23)	1.61	1.64

Table 5 Cooling and heating capacities of typical GEHPs [20]

Parameter	Case 1	Case 2	Case 3	Case 4	Case 5	Case 6	Case 7
Cooling capacity ($\dot{Q}_{eva,c}$) (kW)	14	18	22.4	28	33.5	45	56
Heating capacity ($\dot{Q}_{con,h}$) (kW)	18	23.6	26.5	35.5	42.5	53	67

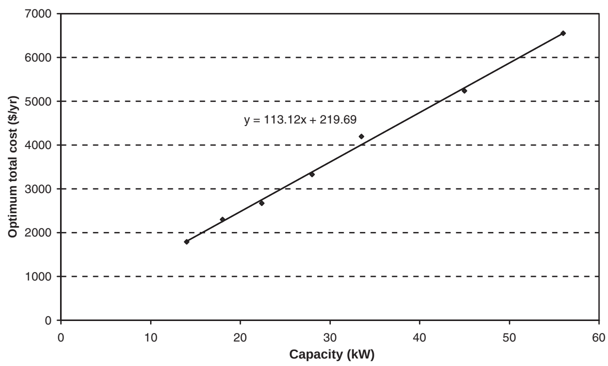

Fig. 6 Optimum values of the total cost for various values of nominal capacity mentioned in Table 5

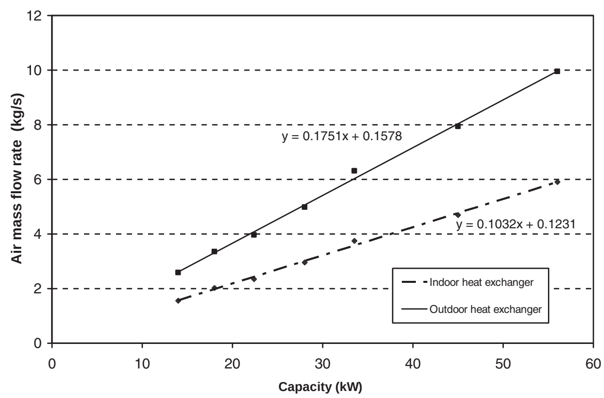

Fig. 8 Air mass flowrate passing through the indoor and outdoor heat exchangers at the optimum design point (the minimum total cost) for various values of nominal capacity mentioned in Table 5

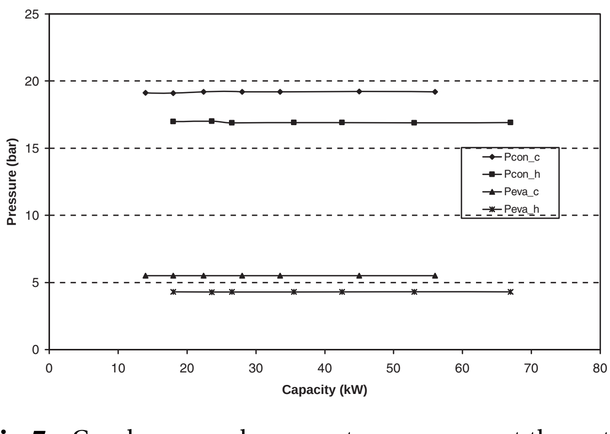

Fig. 7 Condenser and evaporator pressures at the optimum design point (minimum total cost) for various values of cooling/heating capacity mentioned in Table 5

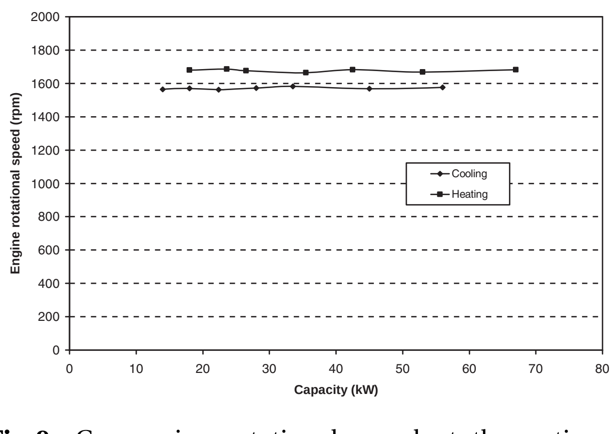

Fig. 9 Gas engine rotational speed at the optimum design point (minimum total cost) for various values of cooling/heating capacity mentioned in Table 5

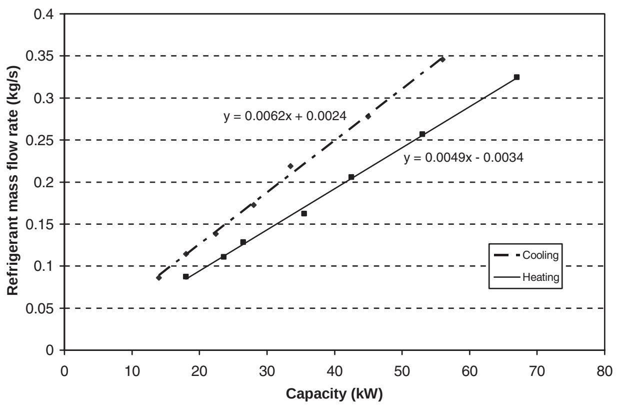

Fig. 10 Refrigerant mass flowrate at the optimum design point (minimum total cost) for various values of cooling/heating capacity mentioned in Table 5

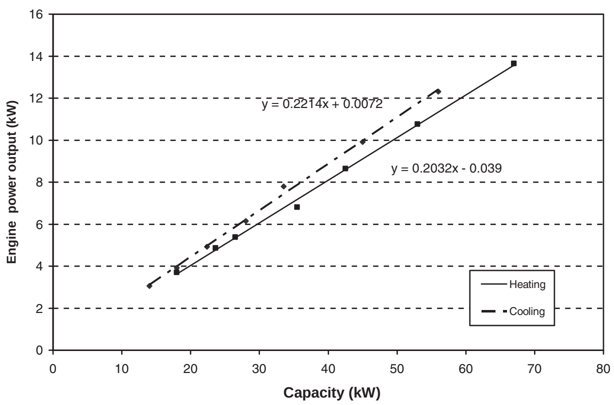

Fig. 11 Engine power output at the optimum design point (minimum total cost) for various values of cooling/heating capacity mentioned in Table 5

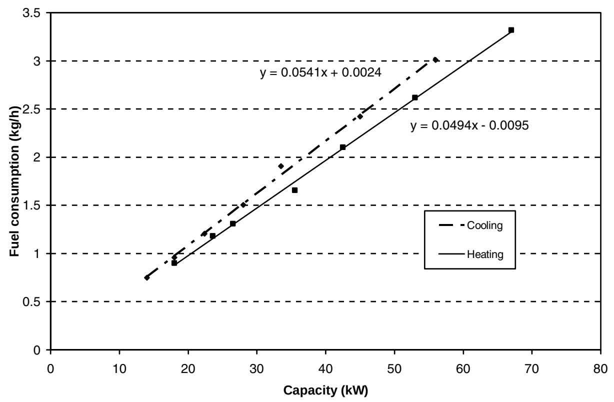

Fig. 12 Fuel consumption at the optimum design point (minimum total cost) for various values of cooling/heating capacity mentioned in Table 5

5.2.1 *Effect of numerical values of design parameters on total cost*

The values of the total cost at the optimum design point are given in Fig. 6. By increasing the cooling capacity (about four times), the minimum total cost increased (about 3.66 times) due to an increase in investment cost (for the bigger size of equipment) as well as an increase in operating cost (due to an increase in the compressor power consumption and gas engine fuel consumption).

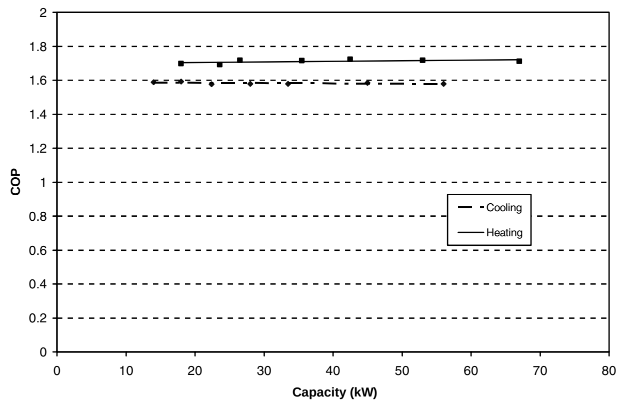

Fig. 13 Coefficient of performance for the GEHP system at the optimum design point (minimum total cost) for various values of cooling/heating capacity mentioned in Table 5

(a) *Evaporator pressure.* Increasing the evaporator pressure in the cooling mode results in the following: a decrease in compressor power consumption and cost (due to a reduction in compressor pressure ratio); a decrease in gas engine investment cost and fuel consumption cost (due to a reduction in compressor power consumption and, accordingly, engine power generation); and a decrease in outdoor heat exchanger cost (due to an increase in condenser efficiency). In this case, the indoor heat exchanger cost increases (due to an increase in its efficiency). The cost of the expansion valve increases slightly (due to an increase in refrigerant mass flowrate). Therefore, considering the superposition of the above effects, the total cost of the system decreases and then increases with increasing evaporator pressure in the cooling mode. The same trend was observed for the heating mode too. Therefore the optimum evaporator pressures at which the minimum total cost was obtained were 5.5 and 4.27 bar in the cooling and heating modes, respectively, as listed in Table 3.

(b) *Condenser pressure.* Increasing the condenser pressure in the cooling mode leads to the following: an increase in compressor investment cost (due to an increase in compressor pressure ratio); an increase gas engine investment cost and fuel consumption cost (due to an increase in compressor power consumption and, accordingly, engine power generation); a decrease in outdoor heat exchanger cost (due to a reduction in condenser efficiency); and no considerable change in indoor heat exchanger cost (because of its unchanged evaporator efficiency) and expansion valve cost (because of the small variation in refrigerant mass flowrate). Therefore, the superposition of the above variations in the cost of components resulted in decreasing and then increasing total cost with increasing condenser pressure in the cooling mode. The same trend was observed for the heating mode too.

Finally, the optimum condenser pressures at which the minimum total cost was obtained were 18.98 bar for the cooling mode and 17.38 bar for the heating mode, as listed in Table 3.

(c) *Air mass flowrate.* It was observed that for a specific heat transfer rate ($\dot{Q}_{\mathrm{ihx}}$) and inlet temperature difference of hot and cold flows ($T_{\mathrm{ihx}} - T_{\mathrm{a,ihx},i}$), the heat exchanger investment cost decreases with increasing air mass flowrate to a minimum point, after which the cost increases smoothly. Furthermore, the increase in air mass flowrate increases continuously the fan electric power consumption. Therefore, at the optimal design point, the sum of two mentioned costs (i.e. $C_{i\mathrm{hx}} + C_{\mathrm{el}}$) showed a minimum value at $\dot{m}_{\mathrm{a,ihx}} = 1.504$ kg/s, which is listed in Table 3.

(d) *Gas engine rotational speed.* Increasing the gas engine rotational speed slightly increases the indicated thermal efficiency (η_{th}) of the engine. This is due to the shorter time period for a thermodynamic cycle and consequently the shorter time period of the expansion (power) stroke that decreases engine heat losses from the cylinder walls. Furthermore, the mechanical efficiency (η_{m}) of the engine showed an increase to a maximum point and then a decrease due to increasing friction effects. The superposition of these effects results in a smooth rise and then fall of the engine brake efficiency ($\eta_{\mathrm{th,b}} = \eta_{\mathrm{ge}} = \eta_{\mathrm{th}}\,\eta_{\mathrm{m}}$) with engine speed (r/min). At the optimal design point, $\eta_{\mathrm{ge}} = 0.348$ was found to be the maximum value of η_{ge} (Table 4) at 1671 r/min, as reported in Table 3.

5.3 Effects of cooling (heating) capacity on the optimum values of design parameters

The investigation of the variation of optimum design parameters at various GEHP nominal cooling capacities mentioned in Table 5 is reported in this section.

Variations in the optimum values of design parameters with cooling and heating capacities (for cases 1 to 7 mentioned in Table 5) are shown in Figs 7 to 9.

Design parameters such as evaporator and condenser pressures (Fig. 7), air mass flowrates in indoor and outdoor heat exchangers (Fig. 8), and gas engine rotational speed (Fig. 9) did not change considerably. However, optimum values of parameters such as refrigerant mass flowrate (Fig. 10), engine power output (Fig. 11), and engine fuel consumption (Fig. 12) increase with an increase in cooling and heating capacities.

The optimum value of the refrigerant mass flowrate increases with an increase in the values of cooling and heating capacities (equations (5) and (8)). This increases compressor power consumption (equation (1)), engine power output (Fig. 11 and equation (16)), and engine fuel consumption (Fig. 12 and equation (18)).

Effective parameters on the COP values were condenser and evaporator pressures and engine thermal efficiency. Since the optimum values of these design parameters did not change considerably with capacity (while compressor power consumption increased with capacity), the COP of the system in cooling/heating modes did not change considerably based on equations (21) and (23). Variations in the optimum values of COP with capacity are shown in Fig. 13.

5.4 Effects of fuel and investment costs on the optimum values of design parameters

The sensitivity analysis of change in the optimum values of design parameters with change in fuel or investment cost is investigated in this section for the case study (ESIL) explained in section 4.

Increasing or decreasing the fuel cost changes the optimum values of design parameters which minimize the objective function.

By increasing the investment cost (for 50 per cent), the optimum value of the evaporator pressure slightly decreased (about 1.45 per cent in heating) and the optimum value of the condenser pressure slightly increased (about 1.49 per cent in cooling and 1.89 per cent in heating modes) to reduce the efficiency of elements (such as efficiency of heat exchangers in equations (32) and (33)) and to compensate the increase in the initial investment.

Decreasing the investment cost of the system resulted in the reverse effects explained above. Therefore, by decreasing the investment cost of elements (for 50 per cent), the evaporator pressure increased (about 2.8 per cent in heating mode) and the condenser pressure decreased (about 3.27 per cent in the cooling mode and 5.53 per cent in the heating mode).

The summary of the effects of change in the fuel and investment cost on the optimum values of design parameters (as well as the total cost values) is presented in Table 6.

5.5 Energy flow diagram

The GEHP system energy flow diagram in optimum cooling and heating modes of operation is shown in

Table 6 Effects of change in the fuel and investment costs on the optimum design parameters for cooling (heating) modes of operation

	Variation in fuel cost (%)		Variation in investment cost (%)	
Parameter	+50 (+25)	−50 (−25)	+50 (+25)	−50 (−25)
$\Delta P_{\mathrm{eva,c}}$ (%)	Negligible change	Negligible change	Negligible change	Negligible change
$\Delta P_{\mathrm{eva,h}}$ (%)	+1.55 (+1.1)	−3.5 (−1.49)	−1.45 (−0.9)	+2.8 (+2.95)
$\Delta P_{\mathrm{con,c}}$ (%)	−2.46 (−1.3)	+3.75 (+1.4)	+1.49 (+0.93)	−3.27 (−1.44)
$\Delta P_{\mathrm{con,h}}$ (%)	−5.58 (−3.77)	+4.14 (+2.34)	+1.89 (+1.04)	−5.53 (−3.24)
$\Delta \dot{m}_{\mathrm{a,ihx}}$ (%)	+12.5 (+8.03)	−6.97 (−4.13)	+0.23 (+0.11)	+4.71 (+3.85)
$\Delta \dot{m}_{\mathrm{a,ohx}}$ (%)	+9.4 (+4.72)	−11.09 (−4.98)	−1.61 (−1.15)	+4 (+1.4)
$\Delta N_{\mathrm{ge,c}}$ (%)	+1.27 (+0.61)	−1.1 (−0.52)	−0.7 (−0.33)	+0.53 (+0.25)
$\Delta N_{\mathrm{ge,h}}$ (%)	+1.5 (+0.73)	−1.35 (−0.71)	−0.78 (−0.36)	+0.67 (+0.32)
ΔC_{tot} (%)	+11.28 (+5.73)	−12.31 (−6.05)	+31.96 (+16.01)	−32.69 (−16.22)

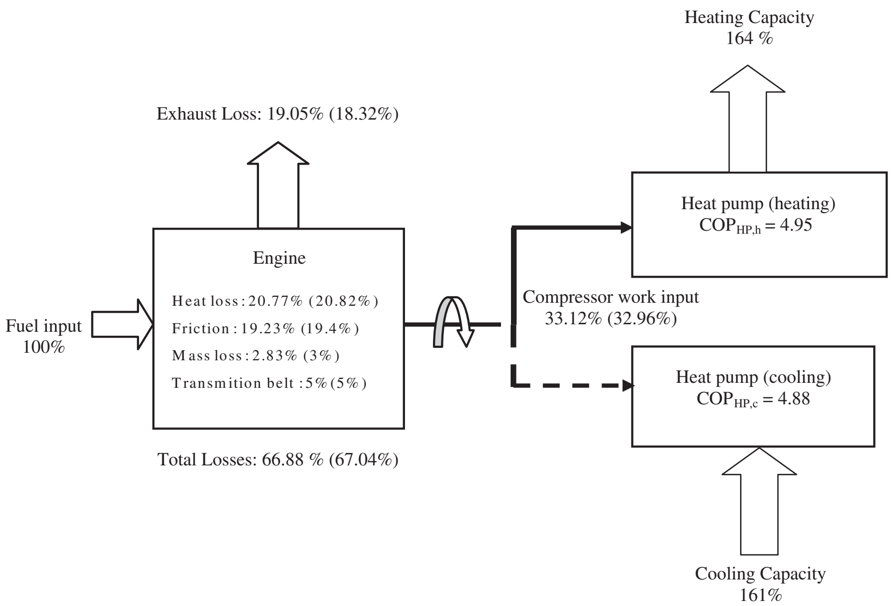

Fig. 14 Energy flow diagram for the GEHP system at the optimum design point (the numbers outside and inside parenthesis are the corresponding values of parameters at the optimum design point of ESIL case study for heating and cooling modes of operation respectively)

Fig. 14. The COP_{HP} in Fig. 14 is the coefficient of performance for the refrigeration cycle (heat pump cycle) defined as the cooling/heating capacity to the compressor power input. The numbers outside and inside parenthesis are the corresponding values of parameters at the optimum design point of ESIL case study for heating and cooling modes of operation respectively.

6 CONCLUSIONS

In this article, modelling and thermal-economic optimization of GEHP systems were performed considering the permissible ranges of design parameters.

The objective function was the sum of the initial investment and operating costs. The selected design parameters were condenser pressure, evaporator pressure, inlet air mass flowrates to the indoor and outdoor heat exchangers, and gas engine rotational speed.

The minimum total cost of the system (the optimum value of the objective function) and the corresponding optimum values of design parameters were computed to provide the required capacity in both cooling and heating modes during a year. The optimization was performed by the GA method exposed to the system constraints.

Also, the effect of change in the numerical values of design parameters on the objective function (the total cost) as well as the variation in the optimal values of design parameters in various cooling and heating capacities were investigated.

The main findings of this study are presented as follows.

1. Correlations for variations in total cost, air mass flowrate, engine power output, fuel consumption, and refrigerant mass flowrate with cooling/heating capacity were proposed for the GEHP system optimum design points. It was observed that there was

no considerable change in the optimum values of evaporator and condenser pressures and rotational speed.
2. By decreasing condenser pressure and increasing evaporator pressure, compressor power consumption as well as compressor and engine investment and the fuel cost decreased, whereas by applying the higher efficiency of the evaporator and condenser, the investment cost of this equipment increased.
3. As a sensitivity analysis, the effects of change in the fuel cost and the initial investment cost on the optimum values of design parameters were studied. By increasing the fuel cost (for 50 per cent), the total cost increased about 11.28 per cent, and by increasing the investment cost (for 50 per cent) the total cost increased about 31.96 per cent. The optimum values of design parameters may change, depending on the regional conditions.
4. In regions at which the fuel price is high, the optimal design procedure reduces the operating cost; however, this increases the efficiency of equipment as well as their investment cost. Therefore, in this situation, the optimum values of the design parameters obtained by the thermal–economic optimization approach are close to the values obtained by the thermal optimization method. In this situation, the minimum fuel consumption and the maximum COP of the heat pump system are desired.
5. The energy flow diagram was illustrated for the whole GEHP system.

REFERENCES

1 **Renedo, C. J., Ortiz, A., Manana, M.,** and **Delgado, F.** A more efficient design for reversible air–air heat pumps. *Energy Build.*, 2007, **39**, 1244–1249.
2 **Zhang, R. R., Lu, X. S., Li, S. Z., Lin, W. S.,** and **Gu, A. Z.** Analysis on the heating performance of gas engine driven air to water heat pump based on a steady state model. *Energy Convers. Manage.*, 2005, **46**, 1714–1730.
3 **Lian, Z., Park, S., Huang, W., Baik, Y.,** and **Yao, Y.** Conception of combination of gas-engine-driven heat pump and water-loop heat pump system. *Int. J. Refrig.*, 2005, **28**, 810–819.
4 **Lazzarin, R.** and **Noro, M.** District heating and gas engine heat pump: economic analysis based on a case study. *Appl. Therm. Eng.*, 2006, **26**, 193–199.
5 **Hepbasli, A., Erbay, Z., Icier, F., Colak, N.,** and **Hancioglu, E.** A review of gas engine driven heat pumps (GEHPs) for residential and industrial applications. *Renew. Sust. Energy Rev.*, 2009, **3**, 85–99.
6 **Nowakowski, G., Metren, G.,** and **Brogan, J.** Field performance of a 3-ton natural gas engine-driven heating and cooling system. *ASHRAE Trans.*, 1995, **2**, 1382–1388.
7 **Yagyu, S., Fujishima, I., Corey, J., Isshiki, N.,** and **Satoh, I.** Design, simulation and test results of a heat-assisted three-cylinder Stirling heat pump (C-3). In Proceeding of the 32nd IECEC, 1997, vol. 2, pp. 1033–1038.
8 **Yagyu, S., Fujishima, I., Fukuyama, Y., Morikawa, T., Obata, N., Corey, J., Isshiki, N.,** and **Satoh, I.** Performance characteristics of a gas engine driven Stirling heat pump. In Proceedings of the AIAA 35th Intersociety Conference, 2000, pp. 85–91.
9 **Wall, G.** Thermoeconomic optimization of a heat pump system, Goteborg, Sweden, Goteborg, S-412 96, September 1985.
10 **Wall, G.** On the optimization of refrigeration machinery. *Int. J. Refrig.*, 1991, **14**, 336–340.
11 **Cammarata, G., Fichera, A. A., Mammino, L.,** and **Marletta, L.** Exergoeconomic optimization of an air conditioning system. *J. Engng Gas Turbines Power*, 1997, **119**, 62–69.
12 **Sanaye, S.** and **Malekmohammadi, H. R.** Thermal and economic optimization of air conditioning units with vapor compression refrigeration system. *Appl. Therm. Eng.*, 2004, **24**, 1807–1825.
13 **Selbas, R., Kızılkan, O.,** and **Sencan, A.** Thermoeconomic optimization of subcooled and superheated vapor compression refrigeration cycle. *Energy*, 2006, **31**, 2108–2128.
14 **Youbi-Idrissi, M., Bonjour, J.,** and **Meunier, F.** Local shifts of the fluid composition in a simulated heat pump using R407C. *Appl. Therm. Eng.*, 2005, **25**, 2827–2841.
15 **Fu, L., Ding, G., Su, Z.,** and **Zhao, G.** Steady-state simulation of screw liquid chillers. *Appl. Therm. Eng.*, 2002, **22**, 1731–1748.
16 **Ferguson, C. R.** *Internal combustion engines*, 1986 (John Wiley, New York).
17 **Heywood, J. B.** *Internal combustion engine fundamentals*, 1988 (McGraw-Hill, New York).
18 **Goldberg, D.** *Genetic algorithms in search optimization and machine learning*, 1996 (Addison-Wesley, Michigan).
19 **Dossat, R. J.** and **Horan, T. J.** *Principles of refrigeration*, 5th edition, 2002 (Prentice Hall, New Jersey).
20 The Installed Gas Heat Pump Service Manual, 2005.
21 **Arora, C. P.** *Refrigeration and air conditioning*, 2000 (Tata-McGraw-Hill, New Delhi).
22 Cooling, Heating, and Power for Buildings (CHP-B) Instructional Module, Mississippi Valley Gas Company and Oak Ridge National Laboratory, Department of Mechanical Engineering, Mississippi State University, 2004.
23 Projected Benefits of Federal Energy Efficiency and Renewable Energy Programs, National Renewable Energy Laboratory, US Department of Energy, 2005.
24 **Humphreys, K. K.** and **Katell, S.** *Basic cost engineering*, 1981 (Marcel Dekker, New York).

APPENDIX 1

Notation

a	annual price coefficient
A	cross-sectional area (m^2)
A_0	inner thermal surface area of the combustion chamber at the top dead centre (m^2)

AF	air to fuel ratio
b	cylinder inner diameter (bore) (m)
c_{el}	electricity price (\$/kW h)
c_{fuel}	fuel price (\$/kW h)
C	elements price (\$/year)
C_0	gas effusion coefficient
C_{el}	cost of power consumption (\$/year)
C_{fuel}	cost of fuel consumption (\$/year)
C_{inv}	initial investment cost (\$/year)
C_{opr}	operating cost (\$/year)
C_p	constant-pressure specific heat (kJ/kg K)
C_{tot}	total annual cost of the system (\$/year)
h	specific enthalpy (kJ/kg)
k	elements cost coefficient
K_{belt}	ratio of the compressor rotational speed to the gas engine rotational speed
m	mass (kg)
$\dot{m}$	mass flowrate (kg/s, kg/h)
n_i	depreciation time of components (year)
N	rotational speed (r/min)
P	pressure (kPa, bar)
q_{LHV}	lower heating value of fuel (kJ/kg)
Q	heat (kJ)
$\dot{Q}$	heat transfer rate (kW)
r	interest rate (per cent)
r_c	compression ratio
R	gas constant (kJ/kg K)
t	time (s)
T	temperature (°C)
v	specific volume (m^3/kg)
V	volume (m^3)
V_0	clearance volume (m^3)
$\dot{V}$	volumetric flowrate (m^3/s)
W	work (kJ)
$\dot{W}$	power (kW)
x	energy emission function
α	convection heat transfer coefficient (kW/m^2 K)
γ	specific heats ratio
η	efficiency
η_{belt}	power transmission efficiency between the engine and the compressor
θ	crank angle (°)
θ_d	duration of heat release
θ_s	crank angle of spark for starting heat release
ρ	density (kg/m^3)
τ	operating time ratio
ω_{ge}	engine frequency (rad/s)

Subscripts

a	air
c	cooling
comb	combustion
comp	compressor
con	condenser
dis	discharge
eff	effective
el	electricity
eva	evaporator
exv	expansion valve
fuel	fuel
ge	gas engine
h	heating
HP	heat pump
i	inlet
ihx	indoor heat exchanger
l	liquid refrigerant
loss	loss
m	mechanical
o	outlet
ohx	outdoor heat exchanger
opr	operating
r	refrigerant
s	isentropic
sub	subcooling
suc	suction
sup	superheating
th	thermal
v	volumetric
w	wall

APPENDIX 2

The compressor cost per unit of time (C_{comp}) was obtained from references [**9**] and [**10**]

$$C_{comp} = a_{comp}\, k_{comp} \frac{V_{comp}}{0.9 - \eta_{comp}} \frac{P_{dis}}{P_{suc}} \ln\left(\frac{P_{dis}}{P_{suc}}\right) \quad (29)$$

The annual costs of indoor (C_{ihx}) and outdoor (C_{ohx}) heat exchangers were estimated from equations (30) and (31) [**9**, **10**]

$$C_{ihx} = a_{ihx}\, k_{ihx}\, \dot{m}_{a,ihx} \left(\frac{\eta_{ihx}}{1 - \eta_{ihx}}\right)^{1/2} \quad (30)$$

$$C_{ohx} = a_{ohx}\, k_{ohx}\, \dot{m}_{a,ohx} \left(\frac{\eta_{ohx}}{1 - \eta_{ohx}}\right)^{1/2} \quad (31)$$

The thermal efficiencies of indoor and outdoor heat exchangers were defined as [**9**, **10**]

$$\eta_{ihx} = \frac{T_{a,ihx,o} - T_{a,ihx,i}}{T_{r,ihx} - T_{a,ihx,i}} \quad (32)$$

$$\eta_{ohx} = \frac{T_{a,ohx,o} - T_{a,ohx,i}}{T_{r,ohx} - T_{a,ohx,i}} \quad (33)$$

The cost of the expansion valve per unit of time (C_{exv}) was defined as

$$C_{exv} = a_{exv}\, k_{exv}\, \dot{m}_r \quad (34)$$

Furthermore, based on the manufacturer's data for the wide range of engine brake power [**22**, **23**], the cost of the gas engine per unit of time (C_{ge}) was obtained as

$$C_{ge} = a_{ge}\left(c_2 \dot{W}_{ge}^2 + c_1 \dot{W}_{ge} + c_0\right) \tag{35}$$

The brake efficiency of the internal combustion gas engine was computed from

$$\eta_{ge} = \eta_{th}\ \eta_{m} \tag{36}$$

The mechanical efficiency of the gas engine was also obtained from curve fitting to the data provided in a series of empirical tests performed on the installed GEHP

$$\eta_{m} = d_2 N_{ge}^2 + d_1 N_{ge} + d_0 \tag{37}$$

Cost coefficients (k) were obtained based on the regional price of elements in the market. a_{comp}, a_{ihx}, a_{exv}, a_{ohx}, and a_{ge} in equations (29) to (31), (34) and (35) represent the annuity factor (a_i) for various equipment, which was defined as [**24**]

$$a_i = \frac{r}{1-(1+r)^{-n_i}} \tag{38}$$

The cost of fuel was presented as

$$\begin{aligned} C_{fuel} &= C_{fuel,c} + C_{fuel,h} \\ &= c_{fuel} t_{opr,c} . \dot{Q}_{fuel,c} + c_{fuel}\ t_{opr,h} . \dot{Q}_{fuel,h} \end{aligned} \tag{39}$$

Subscripts ‘h’ and ‘c’ refer to heating and cooling modes, respectively.

The compressor power consumption and the gas engine power output were related as

$$\dot{W}_{comp} = \eta_{belt}\ \dot{W}_{ge} \tag{40}$$

Substituting the definition of $\dot{W}_{ge} = \eta_{comb}\ \dot{Q}_{fuel}\ \eta_{ge}$ in equation (17), and using equation (36), the relation between compressor power consumption and heat transfer rate from the fuel (fuel heat release) was obtained from

$$\dot{W}_{comp} = \eta_{belt}\ \dot{Q}_{fuel}\ \eta_{comb} . \eta_{m}\ \eta_{th} \tag{41}$$

Therefore

$$\begin{aligned} C_{fuel} = {} & c_{fuel}\ t_{opr,c} \frac{\dot{W}_{comp,c}}{\eta_{belt}\ \eta_{comb}\ \eta_{m}\ \eta_{th,c}} \\ & + c_{fuel}\ t_{opr,h} \frac{\dot{W}_{comp,h}}{\eta_{belt}\ \eta_{comb}\ \eta_{m}\ \eta_{th,h}} \end{aligned} \tag{42}$$

$$C_{el} = C_{el,c} + C_{el,h} = c_{el}\ \dot{W}_{el,c}\ t_{opr,c} + c_{el}\ \dot{W}_{el,h}\ t_{opr,h} \tag{43}$$

The electric power consumption of heat pump fans was related to the system cooling or heating capacity of indoor and outdoor units

$$\dot{W}_{el} = \dot{W}_{el,ihx} + \dot{W}_{el,ohx} \tag{44}$$

The values of electric power consumption of indoor and outdoor units were obtained as a function of air volume flowrate passing through fans, based on the manufacturers’ data

$$\dot{W}_{el,ihx} = e_1 \dot{V}_{a,ihx} + e_2 \tag{45}$$

$$\dot{W}_{el,ohx} = f_1\ \dot{V}_{a,ohx} + f_0 \tag{46}$$